Biochimica et Biophysica Acta 1818 (2012) 1794–1800

Contents lists available at SciVerse ScienceDirect

Biochimica et Biophysica Acta

journal homepage: www.elsevier.com/locate/bbamem

Structure and internal organization of overcharged cationic-lipid/peptide/DNA self-assembly complexes

Jiang Yan [a], Nikolay V. Berezhnoy [a], Nikolay Korolev [a], Chun-Jen Su [b], Lars Nordenskiöld [a,*]

[a] School of Biological Sciences, Nanyang Technological University, 60 Nanyang Drive, Singapore 637551, Singapore
[b] National Synchrotron Radiation Research Center, Hsinchu Science Park, Taiwan

ARTICLE INFO

Article history:
Received 23 December 2011
Received in revised form 15 March 2012
Accepted 30 March 2012
Available online 6 April 2012

Keywords:
Zeta potential
Poisson–Boltzmann model
Polyelectrolyte thermodynamics
Gene delivery

ABSTRACT

The combination of cationic lipids with cationic peptides and DNA vectors can produce synergistic effects in gene delivery to eukaryotic cells. Binary complexes of cationic lipids with DNA are well-studied whereas little information is available about the structure of the ternary lipid/peptide/DNA (LPD) complexes and mechanisms defining DNA protection and delivery. Here we use synchrotron small angle X-ray scattering and dynamic light scattering zeta-potential measurements to determine structure and the net charge of supramolecular aggregates of complexes in mixtures of plasmid DNA, cationic liposomes formed from DOTAP, plus a linear cationic ε-oligolysine with the pendant α-amino acids Leu-Tyr-Arg (LYR), ε-(LYR)K10. These ternary complexes display multilamellar structures with relatively constant separation between DOTAP bilayers, accommodating a hydrated monolayer of parallel DNA rods. The DNA–DNA distance in the complexes varies as a function of the net positive to negative (lipid + peptide)/DNA charge ratio. An explanation for the observed dependence of DNA–DNA distance on charge ratio was proposed based on general polyelectrolyte properties of non-stoichiometric polycation–DNA mixtures.

1. Introduction

Synthetic vector-based gene delivery relying on chemical principles has gained much interest for its safety, biocompatibility and potential for large-scale production [1,2]. Its development offers the potential to circumvent the limitations of viral gene delivery in both basic research laboratories and clinical settings [3]. Phospholipids and peptides are frequently used gene delivery materials [4]. Recently, ternary lipid/peptide/DNA (LPD) complexes have been developed as a promising gene transfer tool [1,5,6]. The improved gene delivery performance of the LPD complex compared to the corresponding binary systems was observed in many cases and studies of the mechanism behind this effect has received much attention [7–12].

Our previous finding suggested that a novel class of synthetic cationic peptides, namely branched ε-oligolysines, based on linear ε-oligolysines with short α-amino acid chains attached to each residue of the main chain (Fig. 1), can cover DNA on the surface of ternary multilamellar complexes of cationic lipids (DOTAP)/ε-oligolysine/DNA [12]. Caracciolo et al. reported that DNA was found at the surface of lipid/DNA particles (lipoplex), while this was not found for lipid/protamine/DNA complexes [11]. In studies of lipoplexes, Oberle et al. found that the imperfection in the lipid/DNA complex formation leads to a partial exposure of plasmid DNA on the surface of the particles [13]. The partial DNA exposure may cause complex clustering and interact with cellular components, thereby inhibiting transfection. Huebner et al. observed this phenomenon for lipoplexes using cryoelectron microscopy as a multilamellar structure with unclosed bilayers at high charge ratio lipid/DNA (lipoplex with open rims of the outer lamellae at low L/D [14]), suggesting that imperfections in lipoplexes occur irrespective of the charge ratio.

Liposomes from cationic phospholipids condense DNA, resulting in a self-assembled complex with ordered structures, which were extensively studied by synchrotron small angle X-ray scattering (SAXS) and shown to influence transfection activities [15–19]. Safinya and co-workers reported that DOTAP/DNA complexes exhibit a multilamellar structure [15]. Inside the complexes, the periodic distance of the multilamellar structure suggested a monolayer of hydrated DNA intercalated between lipid bilayers [15]. Within the layer, the DNA chains are orderly arranged in parallel and give rise to a DNA–DNA correlation peak (q_{DNA}) in SAXS spectra [15]. In our previous study, we found self-assembly of the three components (liposome prepared from DOTAP, ε-oligolysine and DNA) to ordered multilamellar complexes as illustrated in Fig. 2. In the cited work, the charge ratio of lipid DOTAP to DNA (L/D) was fixed and equal to 2 and the charge

Abbreviations: CR, charge ratio; $CR_{+/-}$, charge ratio of positive to negative; d_{DNA}, interaxial DNA–DNA distance; $d_{interlayer}$, interlayer spacing; DLS, dynamic light scattering; DOPE, 1,2-di-(9Z-octadecenoyl)-sn-glycero-3-phosphoethanolamine; DOTAP, 1,2-dioleoyl-3-trimethylammonium-propane; HBS, Hepes-buffered saline; L/D, charge ratio of lipids to DNA; Lipoplex, lipid/DNA complexes; LPD, lipid/peptide/DNA complexes; ε-(LYR)K10: α-substituted ε-K10, the amino acid letters in the brackets denote the substitution groups; P/D, charge ratio of peptides to DNA; SAXS, small-angle X-ray scattering

* Corresponding author. Tel.: +65 6316 2812; fax: +65 6795 3856.
E-mail address: LarsNor@ntu.edu.sg (L. Nordenskiöld).

0005-2736/$ – see front matter © 2012 Elsevier B.V. All rights reserved.
doi:10.1016/j.bbamem.2012.03.022

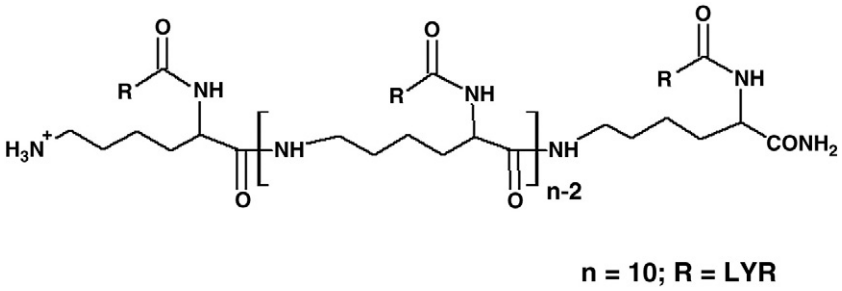

Fig. 1. Chemical structure of α-substituted derivatives of ε-oligolysine ε-(LYR)K10 studied in this work.

ratio of ε-oligolysine to DNA (P/D) was varied in the range of 0.3–5, resulting in overcharged complexes [12]. Peptides distributed in the DNA layer are associated with DNA and contribute to DNA charge neutralization [12]. The structural information was found to be consistent with the observed synergistic effect of DOTAP and ε-oligolysines improving DNA delivery compared to the binary lipid/DNA system [12]. This finding gave an insight about the internal nanostructure of the transfection complex. However, the understanding of the physico-chemical mechanism in formation of the resulting overcharged complexes is still limited.

The dependence of DNA–DNA distance, d_{DNA}, on the positive to negative charge ratio (L/D) was reported for lipid/linear DNA complexes, where either cationic lipid or its mixture with neutral lipids was used [17]. In the present work, the influence of the lipid and peptide composition on the structure of LPD complexes, DOTAP/ε-oligolysine/DNA mixtures with variation of the total lipid + peptide/DNA charge ratio ($CR_{+/-}$) from 1 to 7, was examined by synchrotron small angle X-ray scattering (SAXS). Since both lipids and peptides provide positive charges in the ternary complex, various lipid–peptide mixture compositions are tested, as indicated by the charge ratio lipid/DNA (L/D) and peptide/DNA (P/D). It was found that the DNA–DNA distance in the lamellar structure and the surface charge density (measured by dynamic light scattering zeta potential measurements) of the particles is mainly dependent on the total charge ratio $CR_{+/-}$. For a given $CR_{+/-}$, the DNA–DNA distance is insensitive to the changes of L/D and P/D. It is suggested that the ordered multilamellar structure is maintained by lipid–DNA interaction, whereas the internal organization of the hydrated DNA in the LPD complexes is sensitive to the total balance of positive and negative charges. This implies that peptide molecules are present inside the multilamellar stacks between DNA molecules and that they also influencing the surface charge of the LPD aggregates by association at the surface of the particles. We suggest a simple explanation for the observed variation of d_{DNA} with $CR_{+/-}$ based on an electrostatic analysis of the thermodynamics of non-stoichiometric polycation–polyanion mixtures. This study gives important general information about the physico-chemical mechanism of phospholipid–peptide–DNA self-assembly and contributes to the understanding of the biophysical properties of LPD systems, which aids in further development of these as non-viral gene delivery vehicles.

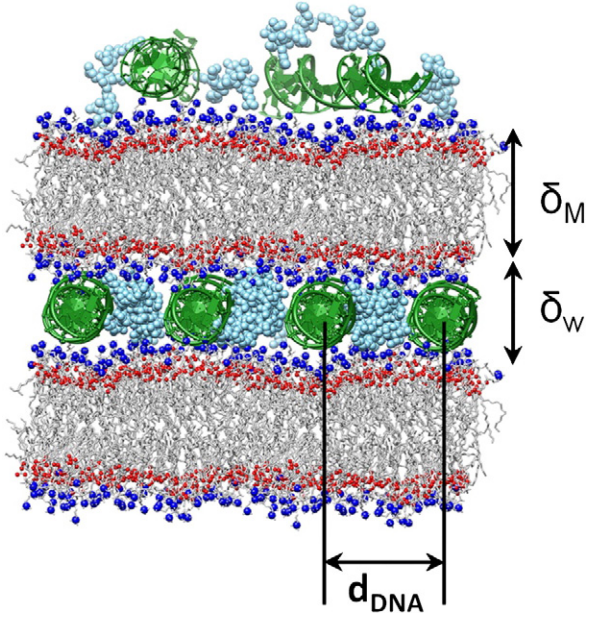

Fig. 2. Schematic picture illustrating the lamellar phase of DOTAP/ε-peptide/DNA complexes, with alternating lipid bilayers and DNA monolayers. Peptides are arranged between DNA chains within the DNA monolayers. The DNA interaxial spacing is dDNA. The interlayer spacing is $d = \delta_m + \delta_w$. The top layer of DNA and peptides associated with the lipid surface illustrates the surface of the overcharged aggregates.

2. Materials and methods

2.1. Materials

2.1.1. DNA

The plasmid pEGFP-N1 (4.7 kbp) encoding the green fluorescent protein GFP was used. The plasmid was amplified in the *Escherichia coli* DH5α strain and extracted by alkaline lysis method. The DNA used in present work was the same as applied for transfection and biophysical studies in our earlier work [10,12].

2.1.2. Peptides

As cationic peptide we used an ε-oligolysine with degree of polymerization 10 and α-amino acid triplet, Leu-Tyr-Arg (LYR) attached to each of the α-amino group of ε-oligolysine, ε-(LYR)K10, (Fig. 1). ε-(LYR)K10 was synthesized using solid-phase peptide synthesis as described in detail in earlier work [10]. The peptide stock solutions (5–25 mg/ml) were prepared in sterile, double-distilled water from lyophilized trifluoroacetic salt. In solutions of neutral pH, amino groups of the ε-(LYR)K10 should be fully protonated and the peptide carries a charge +21e.

2.1.3. Lipids

DOTAP (1,2-dioleoyl-3-trimethylammonium-propane, chloride salt) and DOPE (1,2-di-(9Z-octadecenoyl)-sn-glycero-3-phosphoethanolamine, chloroform) used in SAXS sample preparation were purchased from Avanti Polar Lipids, Inc. (Alabaster, AL, USA). DOTAP solution in chloroform was dried under vacuum at room temperature for 1 h and dissolved in deionized water to concentration 25 mg/ml. Resuspended DOTAP was either extruded by LiposoFast-Basic with 100 nm polycarbonate membrane (Avestin, Inc., Canada) or sonicated with 1 s pulse of 30% amplitude for 10–15 min to clarity by tip sonicator Sonics vibra cell™ (Sonics & Materials Inc., USA). The freshly prepared DOTAP liposomes (mean hydrodynamic diameter of ~100 nm and polydispersity of ~0.1 according to DLS measurement) were stored at room temperature. Liposomes comprised of binary mixture of DOTAP and DOPE are prepared as abovementioned after mixing DOTAP and DOPE chloroform solution at ϕ_{DOPE} (weight fraction) = 0.75.

All other chemicals for buffers were purchased from Fisher Scientific (Pittsburgh, PA, USA).

2.2. Complex preparation

2.2.1. SAXS samples

Lipid/DNA complex was formed by mixing 100 μg plasmid DNA in 75 μl HBS buffer (pH 7.05, 25 mM HEPES, 70 mM NaCl, 0.75 mM Na_2HPO_4) with a proper amount lipids in 75 μl HBS according to the charge ratio lipids to DNA (L/D). Lipid/peptide/DNA complex was formed by combining 100 μg plasmid DNA in 75 μl HBS with the mixture of lipid and peptides in 75 μl HBS, where the amount of lipid and peptide is determined by the charge ratio lipids to DNA (L/D) and charge ratio peptide to DNA (P/D). Since both peptides and lipids carry positive charges, the charge ratio of positive to negative ($CR_{+/-}$) is defined as the sum of the L/D and P/D. The complexes were sealed in 2 mm quartz capillaries (Charles Supper Company, USA) and centrifuged to force precipitates to the bottom of capillaries.

2.2.2. DLS samples

DOTAP/peptide/DNA complexes with the similar formulation to SAXS samples were prepared in a volume of 1 ml for dynamic light scattering (DLS) measurements. The concentration of the complex was optimized for DLS measurement, where DNA was 1.12 μg/ml. Complexes were incubated at room temperature for 30 min prior to DLS measurement.

2.3. Small angle X-ray scattering (SAXS)

SAXS experiments were performed at the Beamline 23A SWAXS endstation at the National Synchrotron Radiation Research Center, Hsinchu (Taiwan) [20]. Data were obtained with 14.0 keV ($\lambda = 0.886$ Å) beam and an area detector (MarCCD165, Mar USA, Evanston, IL) at a sample-to-detector distance of 1.75 m. The scattering wave vector $q = 4\pi\lambda^{-1}\sin\theta$ (with 2θ the scattering angle) was calibrated using silver behenate. SAXS profiles were circularly averaged from the isotropic 2-D patterns measured. All the SAXS data were corrected for background scattering and sample transmission. The ordered distance d was calculated from the q value of the corresponding peak using the relation $d = 2\pi/q$.

2.4. Zeta potential measurement

Zeta potential measurements were done at 25 °C using a Malvern Zetasizer Nano (Malvern Instruments, U.K.) with a laser source operating at a wavelength of 633 nm. The light scattered by the sample was detected at an angle of 17° and zeta potential values were calculated from measured velocities using the Smoluchowski model.

3. Results and discussion

3.1. The charge ratio dependence of the internal organization of lipid/peptide/DNA complexes

The internal structure of the lipid/peptide/DNA (LPD) complexes of various compositions of lipid (DOTAP), peptide (ε-(LYR)K10) and plasmid DNA was studied using synchrotron small-angle X-ray scattering (SAXS). The composition of the LPD mixture is defined by the charge ratios of lipid to DNA (L/D) and peptide to DNA (P/D). The total positive to negative charge ratio, $CR_{+/-}$, is the sum of L/D and P/D. Fig. 3 presents SAXS spectra grouped according to the value of $CR_{+/-}$ for different compositions of DOTAP and ε-(LYR)K10. Binary DOTAP/DNA (LD) complexes were examined for reference and the corresponding SAXS spectra are shown in Fig. 3 at the top of the each panel (black curves) with the LPD spectra below presented in decreasing L/D (increasing P/D) sequence. Spectral characteristics and structural parameter are given in Table S1 of the Supplementary material.

The data in Fig. 3 show that the peaks q_{001} and q_{002} (indicated by black solid arrows in Fig. 3) of the lipid periodic lamellar structures display an interlayer distances $d_{interlayer} = 2\pi n/q_{00n}$ around 59 that is independent of both mixture composition and $CR_{+/-}$. The observed distance is in agreement with a multilamellar structure containing stacked lipid bilayers with intercalated monolayers of hydrated molecules of DNA (the reported thickness of pure DOTAP bilayer is $\delta = 37.2 \pm 0.3$ Å [21]; DNA diameter is ~20 Å). This lamellar distance indicates that for all LPD compositions, the DNA molecules remain in close contact with DOTAP. In addition, there is a peak (q_{DNA}, indicated by pink dashed arrows in Fig. 3) corresponding to the DNA–DNA correlation distance, d_{DNA}, due to parallel ordering of the DNA helices within the aqueous region between the bilayers. The DNA–DNA distance (calculated from the equation $d_{DNA} = 2\pi/q_{DNA}$) varies as a function of the LPD compositions. It is important, however, to note that for the ternary LPD complexes the major determinant of the d_{DNA} value is the total charge ratio of the composition, $CR_{+/-}$. For a given $CR_{+/-}$, q_{DNA} therefore remains unchanged with the variation of L/D and P/D. These results indicate that $CR_{+/-}$ is the major factor determining the internal organization of the lipid/peptide/DNA complexes. Our data is consistent with previous results reported by Koltover et al. [17] and Caracciolo et al. [22].

In Fig. 4, the average values of d_{DNA} calculated for the ternary LPD complexes are plotted as a function of $CR_{+/-}$. The small error bars for each value of d_{DNA} indicate that the DNA–DNA distance is defined by the total charge balance of the LPD mixture ($CR_{+/-}$) with variation of the L/D and P/D ratios. However, d_{DNA} (black squares in Fig. 4) displays two distinct regimes in the range of $CR_{+/-}$. The increase of $CR_{+/-}$ from 1 to 3 results in significant rise of d_{DNA} but the DNA–DNA distance shows little change at $CR_{+/-}$ above 3.

To explain this general behavior we applied a simplified electrostatic approach based on a Poisson Boltzmann polyelectrolyte model developed in previous work to analyze the thermodynamics of non-stoichiometric interactions of the polyelectrolyte DNA with oligocations under conditions of DNA excess [23,24]. In the present work, the LPD mixtures are characterized by an excess of positive charge (lipid + peptide) over the negative charge of DNA charge ($CR_{+/-} > 1$). Hence, the model described in the cited work was changed to the case considering the electrostatic free energy of binding of a negatively charged polyanion (DNA) to positively charged polycations (lipid/peptide), where the positive polycation is in excess. A detailed description of the method and calculated results is given in the Supporting Text 1 of the Supplementary material.

Although this approach is simplified, it nevertheless gives a clear indication that the interaction of all available polycations (cationic lipids plus peptides) with a polyanion like DNA, results in significant gain of electrostatic free energy (Δg^{el}). The important conclusion is that elevated values of the charge ratio, $CR_{+/-}$ (in the range 1–3), results in a significant decrease in electrostatic free energy (about 50% reduction) compared to the initial Δg^{el}, observed for a stoichiometric (1:1) complex with $CR_{+/-} = 1$ (Fig. S1 of the Supplementary material). We suggest that this simplified analysis explains the increase in DNA–DNA distance in the lamellar phase of the LPD complexes since insertion of peptides between DNA molecules, allows interaction of a maximal amount of positively charged species with the polyanion. Fig. S1 also shows that the major effect is reached for $CR_{+/-}$ values between 1 and 2; but there is additional decrease of Δg^{el} for $CR_{+/-}$ values between 2 and 3. Furthermore, for $CR_{+/-} > 3$, further addition of polycation does not noticeably facilitate binding to DNA. The trend in the calculated electrostatic free energy matches very well the experimentally observed increase of d_{DNA} and surface charge (see below) for the particles as a function of charge ratio, $CR_{+/-}$ (Fig. 4).

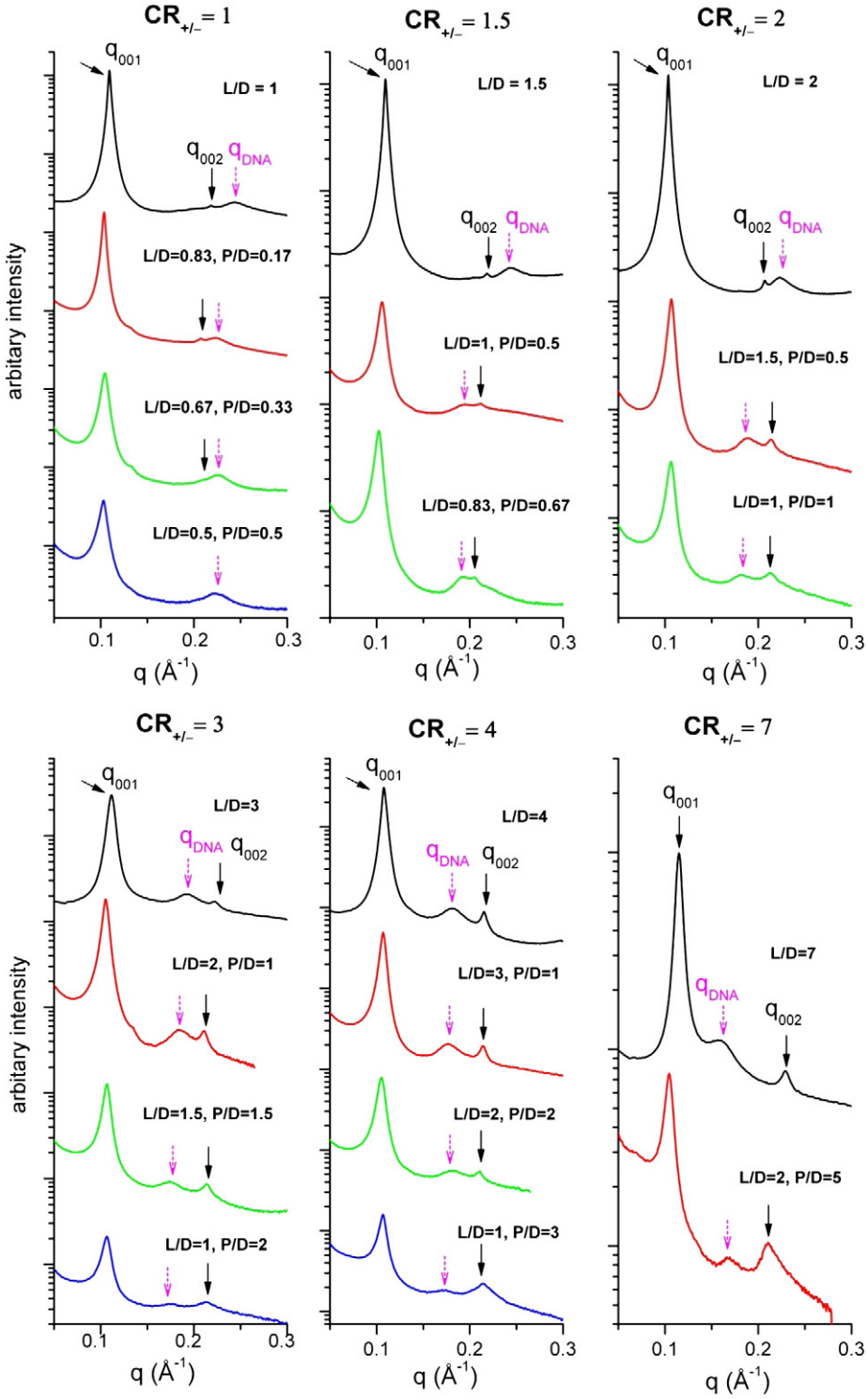

Fig. 3. Synchrotron SAXS scans of the complexes DOTAP/DNA, DOTAP/ε-(LYR)K10/DNA at low (1; 1.5; 2) and high (3.0; 4.0; 7.0) total positive (peptide + DOTAP) to negative (DNA) charge ratio, $CR_{+/-}$, determined for different proportions of peptide and lipid in the mixtures (indicated in the graphs). Black solid arrows indicate the lipid lamellar peaks; pink dashed arrows indicate the DNA–DNA correlation peaks.

The results of this simplified theoretical analysis based on numerical solution of the Poisson Boltzmann (PB) equation are in agreement with similar considerations by Koltover et al. [17]. These authors used a related approach estimating d_{DNA} from an analytical solution of the PB equation under simplified assumptions. The observations of saturation for a system with reversed charge stoichiometry (with excess of oligocations) indicate a general polyelectrolyte behavior of polycation/polyanion mixtures. These authors, however, suggested that the limitation of intake of excess cationic lipids may be due to electrostatic repulsion between the lipid bilayers. They argued that since the interaction between DNA and lipids overcome the electrostatic repulsion between lipid bilayers to form the multilamellar stacks [15], the limitation of the d_{DNA} growth keeps complexes away from disassembly. Our analysis suggests that the effect of saturation of the DNA–DNA distance might be due to a purely thermodynamic

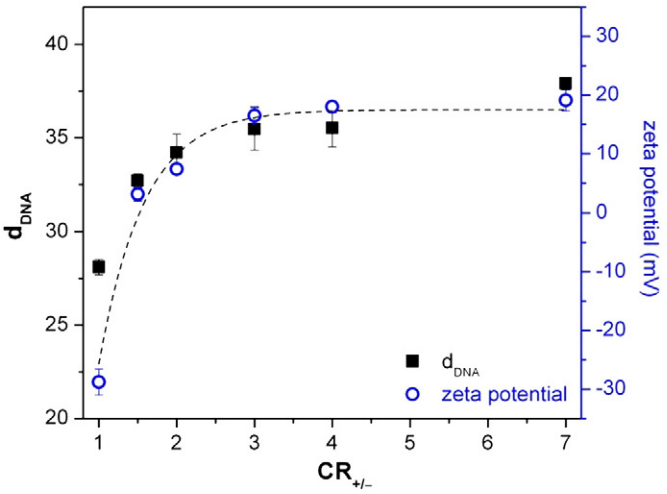

Fig. 4. Dependence of d_{DNA} (black squares) and zeta potential (blue circles) of LPD complex as a function of total (ε-(LYR)K10 + DOTAP)/DNA charge ratio, $CR_{+/-}$. Blue circles denote the average zeta potentials calculated from all the formulations at a certain $CR_{+/-}$. Black squares are the average d_{DNA} of the LPD complexes with various formulations at a fixed $CR_{+/-}$ shown in Fig. 3. The dash line is guide to the eye. The error bars were obtained by averaging the values of zeta potentials and d_{DNA} values observed for different LPD formulations.

effect, caused by the fact that the gain in electrostatic free energy upon cation–DNA association will ceases for $CR_{+/-} > 3$.

A difference between our data and the results obtained by Safinya and co-workers [17] is that we observed a gradual increase of d_{DNA} with increase of $CR_{+/-}$ only in the ternary LPD mixtures. The binary DOTAP/DNA formulations (where L/D = $CR_{+/-}$, P/D = 0) showed a different dependence of d_{DNA} on $CR_{+/-}$ (compared to the LPD complexes): namely, a moderate change of d_{DNA} with $CR_{+/-}$ was observed for L/D<3; and only at high $CR_{+/-}$ values 4–7, did DNA–DNA distance become comparable to the d_{DNA} observed in the ternary LPD mixtures at the same $CR_{+/-}$ (top spectra in each panel of Fig. 3; Table S1). We suggest that this discrepancy has its origin in the nature of the DNA applied in our study. We used supercoiled plasmid DNA, whereas linear DNA was studied by Koltover et al. The ε-oligolysines are capable of penetrating between the chains of the supercoiled DNA, while the cationic groups of DOTAP are restricted in their mobility being confined in the lipid bilayer. Hence, a larger excess of lipid cationic charge is required in the binary L/D systems.

3.2. Correlation between surface charge and d_{DNA}

In addition to the SAXS studies of the internal structure, the zeta potential of LPD complexes was determined for the same DOTAP–ε-oligolysine–DNA formulations. In Fig. 4, d_{DNA} values from the SAXS study are combined with the values of zeta potentials and plotted as a function of $CR_{+/-}$. For each given $CR_{+/-}$, similar values of zeta potentials were observed for the LPD complexes differing in the L/D and P/D values as indicated by small error bars in Fig. 4. LPD complexes are negatively charged (~−28.8 mV) at $CR_{+/-} = 1$ but the zeta potential reverses the sign to ~+3 mV when $CR_{+/-}$ increases to 1.5. With further increase of $CR_{+/-}$, a continuous rise is followed by a plateau at ~+17 mV at $CR_{+/-} > 3$, implying that the positive charge on the surface is saturated at $CR_{+/-} > 3$.

Fig. 4 clearly shows that the variation of the surface potential and the change in d_{DNA} inside the LPD complexes have similar dependence on $CR_{+/-}$. The increase in the DNA–DNA distance upon change of $CR_{+/-}$ from 1 to 3 is accompanied by a significant increase in the zeta potential and a reverse in sign from negative to positive. These results indicate that the positive molecules are incorporated inside the complex as well as being present on the surface. The plateau at $CR_{+/-} > 3$ for both d_{DNA} and zeta potential suggests that the association of positive molecules tends to be saturated at $CR_{+/-} = 3$.

The zeta potential values determined in this work are in agreement with the measurements reported in our previous work [12]. Specifically, we observed that the change of sign of the zeta potential from negative to positive, is found at higher value of $CR_{+/-}$ compared to the work that studied interaction between cationic lipids and DNA at low concentration of salt [17]. In the cited work, the zeta potential changed sign at $CR_{+/-}$ close to the point of the electroneutrality ($CR_{+/-} = 1$). In the present work, we use higher salt concentration to mimic the conditions of the transfection experiment (25 mM Hepes, pH 7.05, 70 mM NaCl, and 0.75 mM Na_2HPO_4). This cation concentration (below 100 mM) is not sufficient to enable efficient competition with the ε-oligolysines for binding to DNA [25], but it is high enough for Na^+ ions to affect lipid–DNA binding. Under such salt conditions (at $CR_{+/-}$ about 2), complexes of DNA with cationic vectors have a negative zeta-potential [7,9,26]. Therefore, this difference in sign of the zeta potential could be explained by the competition between lipids and monovalent cations for neutralization of the negative charge of the DNA molecules that are absorbed on the surface of the particles (as discussed in detail in our earlier work [12]).

3.3. The effect of lipid–peptide composition on the internal organization of lipid/peptide/DNA complexes

Although the internal structure of DOTAP/DNA is similar to DOTAP/peptide/DNA complexes (Fig. 2), the values of d_{DNA} at $CR_{+/-} = 1.5$ and 2 are larger in the presence of peptide. The composition of the positive molecules may influence the internal structure in addition to the total $CR_{+/-}$. In Fig. 3 at $CR_{+/-} = 1$, 1.5 and 2 all LPD compositions contain high lipid proportion, so that at least 50% the total positive charge is provided by DOTAP and L/D ≥ P/D. To illustrate the influence of the relative amounts of the peptide and lipid on the LPD structure, complexes with low lipid proportion (L/D<P/D) at $CR_{+/-} = 1$, 1.5 and 2 were additionally studied. Fig. 5 shows the SAXS spectra of complexes containing a low lipid proportion, i.e. DOTAP contributes less than 50% of the total positive charge. Spectral characteristics and structural parameter are summarized in Table S2.

At $CR_{+/-} = 1$, the signal intensity of the first lamellar peak q_{001} is significantly reduced for L/D = 0.33, and the lamellar peaks almost vanish for L/D = 0.17 (Fig. 5). This result shows that lipids are the major building blocks to maintain the ordered multilamellar stacks. At $CR_{+/-} = 1.5$, the LPD complexes containing low lipid proportion, exhibit similar diffraction patterns as recorded for complexes with higher L/D (shown in Fig. 3). However, there is an extra peak at $q^* = \sim 0.219\ Å^{-1}$. This peak probably originates from a compact packing of DNA chains corresponding to a d_{DNA}^* of ~28.7 Å originating from DNA condensed by peptides in lipid-free aggregates. Ordered structure with a peak at a similar position can be observed for peptide/DNA complex without lipids at a peptide to DNA ratio, P/D = 1. Under these conditions, aggregates are formed and visually seen in the solution that give rise to a weak peak in SAXS spectra that is likely to originate from the DNA–DNA correlation in condensed DNA [27] (see Supplementary material; Fig. S2). This suggests that two phases with different DNA packing regimes (d_{DNA}^* ~28.7 Å and d_{DNA} ~33 Å) coexist at low L/D for the LPD systems. The phase with the larger DNA–DNA spacing is similar to the observations for LPD complexes at high L/D in Fig. 3 and suggested to be a ternary complex, while the aggregate with shorter DNA–DNA separation is attributed to DNA condensed by peptides. The coexistence of the two phases with different q_{DNA} also occurs for $CR_{+/-} = 2$ (d_{DNA}^* ~29.3 Å and d_{DNA} ~34 Å). However, we did not note the presence of lipid-free peptide–DNA complexes which was observed at high $CR_{+/-}$, probably because the amount of lipid is sufficient to include all available DNA in the multilamellar phase.

Although DNA, polycations and cationic lipids can form a ternary complex in a variety of formulations (with $CR_{+/-} = 1$–7), an excess

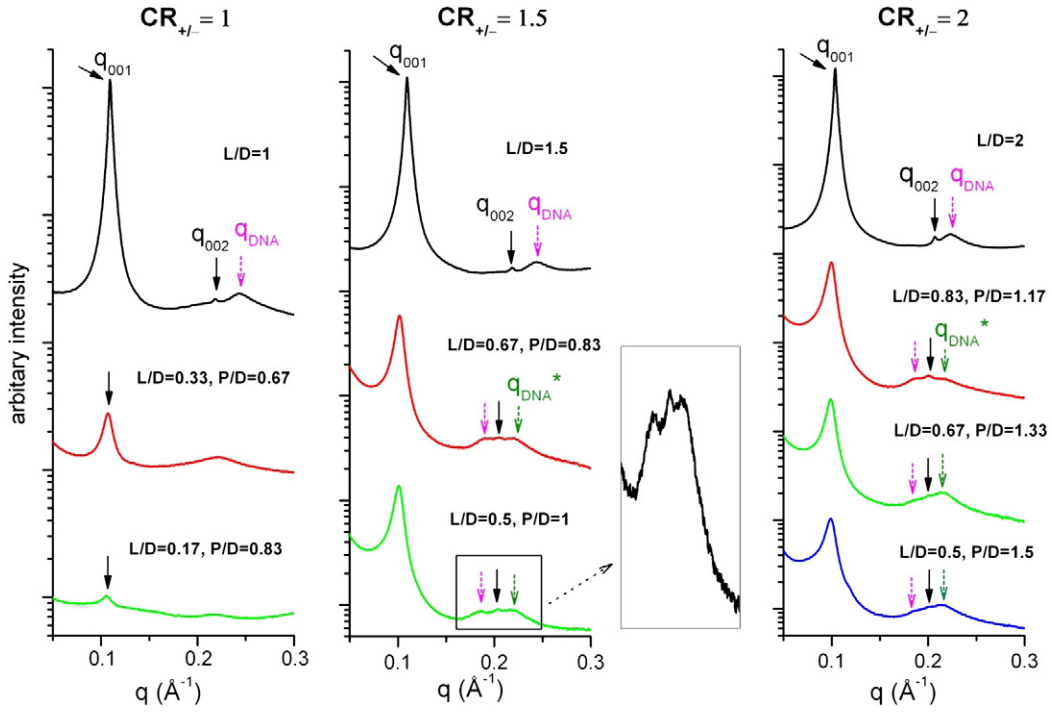

Fig. 5. Synchrotron SAXS scans of the complexes DOTAP/ε-(LYR)K10/DNA at total $CR_{+/-}$ (1, 1.5 and 2) determined for a low proportion of lipid in the mixture (indicated in the graphs). Black solid arrows indicate the lipid lamellar peaks; pink dashed arrows indicate the DNA–DNA correlation peaks. The green arrows denote the peak attributed to DNA–DNA correlation in the ε-peptide/DNA complex, indicated as q_{DNA}^*. The inset is the enlarged graph of the spectra in the box.

of cationic lipids and polycations (L/D > 1, P/D > 1) may be necessary for successful gene delivery. It is well recognized that a large excess of positively charged vectors is needed to mediate optimal gene transfer [1]. In LPD systems, a sufficient amount of lipids is essential for structuring of the complex. The necessity of an excessive amount of the polycations is indicated in our earlier study where a significant enhancement of the transfection was been observed for the ternary formulations compared to the binary ε-peptides–DNA or DOTAP–DNA recipes [12]. Since the major increase in surface charge is found for $CR_{+/-} < 3$, we suggest that $CR_{+/-} > 3$ might be used in more directed search for efficient gene delivery formulations.

4. Conclusions

The nanostructures of DOTAP/ε-oligolysine/DNA complexes were investigated by synchrotron SAXS and dynamic light scattering zeta potential methods for varying composition of lipid and peptide in a broad range of charge ratio, $CR_{+/-}$. These ternary complexes display multilamellar structures, in which interlayer spacing is largely insensitive to the composition of the mixture (~59 Å). It was observed that the separation between the DNA double helices inside the hydration layer of the multilamellar structure, d_{DNA}, increases significantly with the increase of $CR_{+/-}$ in the range 1–3. Further $CR_{+/-}$ increase above three does not influence d_{DNA}. The DNA–DNA distance correlates with the surface charge of the LPD aggregates (Fig. 4). According to a thermodynamic analysis, the $CR_{+/-}$ dependence can be explained by the gain in free energy due to the interaction of the DNA with the maximal possible positive amount of lipid plus peptide charge. This effect is most significant at low charge ratios, for $CR_{+/-}$ in the range 1–3.

Acknowledgements

This work was financially supported by the Singapore Agency for Science Technology and Research (A*STAR) BMRC (Biomedical Research Council) grant and by Singapore Ministry of Education (MOE) Tier 2 and ARC-Tier 1 grants. The National Synchrotron Radiation Research Center (NSRRC) at Hsinchu, Taiwan is acknowledged for generous allocation of beamtime that enabled the Synchrotron X-Ray scattering measurements. We are indebted to the Small/Wide Angle X-ray Scattering beamline staff for technical assistance.

Appendix A. Supplementary data

Supplementary data to this article can be found online at doi:10.1016/j.bbamem.2012.03.022.

References

[1] X. Gao, K.-S. Kim, D. Liu, Nonviral gene delivery: what we know and what is next, AAPS J. 9 (2007) E92–E104.
[2] P. Saccardo, A. Villaverde, N. González-Montalbán, Peptide-mediated DNA condensation for non-viral gene therapy, Biotechnol. Adv. 27 (2009) 432–438.
[3] M.A. Mintzer, E.E. Simanek, Nonviral vectors for gene delivery, Chem. Rev. 109 (2009) 259–302.
[4] T. Segura, L.D. Shea, Materials for non-viral gene delivery, Annu. Rev. Mater. Res. 31 (2001) 25–46.
[5] X. Gao, L. Huang, Potentiation of cationic liposome-mediated gene delivery by polycations, Biochemistry 35 (1996) 1027–1036.
[6] F.L. Sorgi, S. Bhattacharya, L. Huang, Protamine sulfate enhances lipid-mediated gene transfer, Gene Ther. 4 (1997) 961–968.
[7] K.K. Son, D. Tkach, D.H. Patel, Zeta potential of transfection complexes formed in serum-free medium can predict in vitro gene transfer efficiency of transfection reagents, Biochim. Biophys. Acta 1468 (2000) 11–14.
[8] Q.R. Chen, L. Zhang, S.A. Stass, A.J. Mixson, Branched co-polymers of histidine and lysine are efficient carriers of plasmids, Nucleic Acids Res. 29 (2001) 1334–1340.
[9] L. Hyndman, J.L. Lemoine, L. Huang, D.J. Porteous, A.C. Boyd, X. Nan, HIV-1 Tat protein transduction domain peptide facilitates gene transfer in combination with catioinc liposomes, J. Control. Release 99 (2004) 435–444.
[10] D. Huang, N. Korolev, K.D. Eom, J.P. Tam, L. Nordenskiöld, Design and biophysical characterization of novel polycationic ε-peptides for DNA compaction and delivery, Biomacromolecules 9 (2008) 321–330.
[11] G. Caracciolo, D. Pozzi, A.L. Capriotti, C. Marianecci, M. Carafa, C. Marchini, M. Montani, A. Amici, H. Amenitsch, M.A. DIgman, E. Gratton, S.S. Sanchez, A. Lagana, Factors determining the superior performance of lipid/DNA/protammine nanoparticles over lipoplexes, J. Med. Chem. 54 (2011) 4160–4171.
[12] J. Yan, N. Korolev, K.D. Eom, J.P. Tam, L. Nordenskiöld, Biophysical properties and supramolecular structure of self-assembled liposome/ε-peptide/DNA nanoparticles: correlation with gene delivery, Biomacromolecules 13 (2012) 124–131.

[13] V. Oberle, U. Bakowsky, I.S. Zuhorn, D. Hoekstra, Lipoplex formation under equilibrium conditions reveals a three-step mechanism, Biophys. J. 79 (2000) 1447–1454.
[14] S. Huebner, B.J. Battersby, R. Grimm, G. Cevc, Lipid–DNA complex formation: reorganization and rupture of lipid vesicles in the presence of DNA as observed by cryoelectron microscopy, Biophys. J. 76 (1999) 3158–3166.
[15] J.O. Rädler, I. Koltover, T. Salditt, C.R. Safinya, Structure of DNA–cationic liposome complexes: DNA intercalation in multilamellar membranes in distinct interhelical packing regimes, Science 275 (1997) 810–814.
[16] I. Koltover, T. Salditt, J.O. Rädler, C.R. Safinya, An inverted hexagonal phase of cationic liposome–DNA complexes related to DNA release and delivery, Science 281 (1998) 78–81.
[17] I. Koltover, T. Salditt, C.R. Safinya, Phase diagram, stability, and overcharging of lamellar cationic lipid–DNA self-assembled complexes, Biophys. J. 77 (1999) 915–924.
[18] A.J. Lin, N.L. Slack, A. Ahmad, I. Koltover, C.X. George, C.E. Samuel, C.R. Safinya, Structure and structure–function studies of lipid/plasmid DNA complexes, J. Drug Target. 8 (2000) 13–27.
[19] C.R. Safinya, Structures of lipid–DNA complexes: supramolecular assembly and gene delivery, Curr. Opin. Struct. Biol. 11 (2001) 440–448.
[20] U.S. Jeng, C.H. Su, C.J. Su, K.F. Liao, W.T. Chuang, Y.H. Lai, J.W. Chang, Y.J. Chen, Y.S. Huang, M.T. Lee, K.L. Yu, J.M. Lin, A small/wide-angle X-ray scattering instrument for structural characterization of air–liquid interfaces, thin films and bulk specimens, J. Appl. Crystallogr. 43 (2010) 110–121.
[21] J. Rädler, I. Koltover, A. Jamieson, T. Salditt, C.R. Safinya, Structure and interfacial aspects of self-assembled cationic lipid–DNA gene carrier complexes, Langmuir 14 (1998) 4272–4283.
[22] G. Caracciolo, D. Pozzi, R. Caminiti, H. Amenitsch, Formation of overcharged cationic lipids/DNA complexes, Chem. Phys. Lett. 429 (2006) 250–254.
[23] N. Korolev, A.P. Lyubartsev, A. Laaksonen, Electrostatic background of chromatin fiber stretching, J. Biomol. Struct. Dyn. 22 (2004) 215–226.
[24] N. Korolev, A.P. Lyubartsev, L. Nordenskiöld, Application of the Poisson Boltzmann polyelectrolyte model for thermal denaturation of DNA in the presence of Na^+ and polyamine cations, Biophys. Chem. 104 (2003) 55–66.
[25] N. Korolev, N.V. Berezhnoy, K.D. Eom, J.P. Tam, L. Nordenskiöld, A universal description for the experimental behavior of salt-(in)dependent oligocation-induced DNA condensation, Nucleic Acids Res. 37 (2009) 7137–7150.
[26] D. Li, Y. Ping, F. Xu, H. Yu, H. Pan, H. Huang, Q. Wang, G. Tang, J. Li, Construction of a star-shaped copolymer as a vector for FGF receptor-mediated gene delivery in vitro and in vivo, Biomacromolecules 11 (2010) 2221–2229.
[27] C.-J. Su, H.-L. Chen, M.-C. Wei, S.-F. Peng, H.-W. Sung, V.A. Ivanov, Columnar mesophases of the complexes of DNA with low-generation poly(amido amine) dendrimers, Biomacromolecules 10 (2009) 773–783.